Nondestructive Evaluation and Microfailure Modes of Single Fibers/Cement Composites using Electro-Micromechanical Technique and Acoustic Emission

Sang-Il Lee[*], Jin-Won Kim[*], Joung-Man Park[*,†], Dong-Jin Yoon[**]

Electro-Micromechanical 시험법과 음향방출을 이용한 단섬유시멘트복합재료의 미세파괴구조와 비파괴적 평가

이상일[*] · 김진원[*] · 박종만[*,†] · 윤동진[**]

KEY WORDS: electro-micromechanical technique, contact resistivity, dual matrix composite (DMC), interfacial shear strength (IFSS), acoustic emission (AE), nondestructive (NDT) evaluation

ABSTRACT

The contact resistivity was correlated with IFSS and microfailure modes in conductive fiber/cement composites electro-pullout and AE. As IFSS increased, the number of AE signals increased and the contact resistivity increased latter to the infinity. In dual matrix composite (DMC) test and AE, the number of signals with high amplitude and energy in glass fiber composite is significantly larger than that of no-fiber composite. Many vertical and diagonal cracks were observed in glass fiber and no-fiber composite under tensile test, respectively. Electro-micromechanical technique and AE can be used efficiently for sensitive nondestructive (NDT) evaluation and to detect microfailure mechanisms in various conductive fibers reinforced brittle and nontransparent cement composites.

Nomenclature

τ_i, τ : IFSS of electro-pullout and DMC composites
F_d : The maximum pullout force
σ_{mu} : The stress at which the crack begins to form
x : Crack spacing of brittle matrix
R_v, ρ_v: Volume resistance and resistivity
R_c, ρ_c: Contact resistance and resistivity

1. INTRODUCTION

Microfailure mechanisms of cement matrix composite (CMC) are basically different from fiber reinforced plastic (FRP) composites. The toughness of fiber reinforced CMC is much higher than brittle ceramic materials. The toughness mechanism is provided by fiber bridging in the plane of a matrix crack. Regarding fiber reinforced brittle CMC, many theory and models of matrix crack mechanism have been studied using micromechanical techniques [1,2]. DMC technique [3] is basically modified from the single fiber composite (SFC) test. DMC specimen, chosen to evaluate microfailure modes and interfacial properties, is composed of a single fiber, a brittle layer (inner matrix for measuring IFSS) and ductile matrix (supportable outer matrix). Single fiber Broutman test [4] was recently used to investigate interface properties and microfailure mechanism. This technique, which is based on the compression of a single fiber necked specimen, was performed to apply a transverse stress to the interface. AE is well-known as one of the important NDT methods [5]. During the fracture progressing, the AE can monitor the fracture behavior of composite materials, and can characterize many AE parameters to understand the type of microfailure sources such as fiber fracture, matrix cracking, and debonding at the fiber-matrix interface. Single fiber electro-pullout test was reported initially by Chung *et al.* [6]. To provide the information on the

[*] Department of Polymer Science and Engineering, Research Center for Aircraft Parts Technology, Gyeongsang National University
[**] Nondestructive Evaluation Group, Korea Research Institute of Standard and Science,
[†] To whom correspondence should be addressed

interfacial adhesion and microfailure modes, the contact resistivity of steel fiber/cement matrix composites was measured. The contact resistivity was correlated to interfacial adhesion as a function of fiber surface treatment. In the untreated and treated fiber reinforced brittle cement composites, nondestructive characteristics and microfailure modes were evaluated using electro-micromechanical technique and AE.

2. EXPERIMENTAL

2. 1. Materials

Carbon fiber with diameter of 18 ㎛ (Mitsubishi Chemical Co., Japan), steel fiber with diameter of 280 ㎛ and glass fiber with diameter of 125 ㎛ were used. Early strength Portland cement (Type Ⅲ, Ssangyong Cement Industrial Co., Korea) was used as an inner brittle matrix. For preparing DMC specimen, an outer matrix was made of the mixture of epoxy resin (YD-128, Kukdo Chemical Co., Korea) based on diglycidyl ether of bisphenol-A (DGEBA) and polyoxypropylene diamine curing agents (Jeffamine D-400 and D-2000, Huntzman Petrochemicals Co.). Matrix modulus was adjusted properly by relative mixing proportion of D-400 *versus* D-2000 in order to obtain the optimum ductility for electro-micromechanical testing. For fiber surface treatment, Neoalkoxy zirconate (Zr, NJ-38J, Kenrich Petro-chemicals Inc.) was used as a coupling agent.

2. 2. Methodologies

2. 2. 1. Fiber Surface Treatment and Testing Specimen Preparation: Three fibers were dipped into 7 wt% Zr coupling agent/ethanol solution for 2 minutes. Some steel fiber was treated by hand-sanded method with sand paper (#400) to enhance the mechanical interlocking. For electro-micromechanical pullout test, the single steel fiber/cement composite exhibits in Figure 1(a). Figures 1(b) and (c) show two types of DMC specimens that were composed of single glass fiber/cement/epoxy for tensile/compressive tests and AE. Single fiber cement composite was cured at 25 °C, 90 % humidity for 3 days.

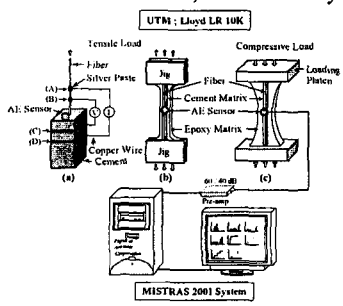

Fig. 1 Testing specimens and experimental system.

In DMC, cement paste was coated on the glass fiber. Just after curing process, glass fiber/thin cement composite was fixed in the silicone mold. After epoxy mixture was poured into the mold, epoxy was precured at 80 °C for 2 hours and then postcured at 120 °C for 2 hours.

2. 2. 2. IFSS and Microfailure Modes Measurements: The electro-pullout specimen strained incrementally and tensile load was applied until fiber was pulled out completely from cement matrix. The shear force developed at the interface between conductive fiber and matrix was measured during single fiber electro-pullout test. IFSS of microspecimen can be derived from the maximum pullout force (F_d) using following equation:

$$\tau_i = \frac{F_d}{\pi d L} \tag{1}$$

Where d and L are fiber diameter and fiber embedded length in the cement, respectively. IFSS and microfailure modes of DMC specimen were measured using UTM and a polarized-light microscope during tensile/compressive testing. When DMC specimen is stressed in tension parallel to the fiber length, multiple fracture of brittle cement matrix can occur, and the fiber can endure the applied stress when the matrix fails. The relationship between IFSS, τ and matrix crack spacing, x, is given by the following equation

$$x = \frac{V_m \sigma_{mu} d}{2 V_f \tau} \tag{2}$$

Where V_m and V_f are the volume fraction of the matrix and fiber, respectively. d is the fiber diameter and σ_{mu} is the stress at which the crack begins to form.

2. 2. 3. Resistivity Properties Measurement: The resistivity properties of single fiber/cement composite were measured by the well-known four-probe method. Silver paste was used as an electrically connecting glue at 4 junctions for maintaining electrical contact between the microspecimen and leading wires (Figure 1). The electrical resistivity of a bare fiber was obtained from the measured electrical resistance, the cross-sectional area of the conductive fiber, A, and electrical contact length, L_{ec} between voltage contacts. The relationship between the electrical resistivity, ρ and resistance, R is as follows:

$$\rho = \left(\frac{A}{L_{ec}} \right) \times R \tag{3}$$

Total electrical resistance, R_{tot} between B and C may include R_s based on contact resistance by silver paste plus R_f due to the resistance by fiber as follows:

$$R_{tot} = R_s + R_f \tag{4}$$

Since the values of R_s are negligibly small due to very high conductivity of silver paste comparing to R_f, it can be considered that the voltage developed between junction B and C reflects nearly fiber resistance,

$$R_{tot} \cong R_f \quad (5)$$

The contact resistivity of conductive fiber/cement composite can be different from that for the electrical resistivity of a bare fiber. Contact resistance, R_c and volume resistance, R_v are related to the contact resistivity, ρ_c and volume resistivity, ρ_v, respectively.

$$R_c = \frac{\rho_c}{A_c}, \qquad R_v = \rho_v \frac{l}{A_v} \quad (6), (7)$$

Where A_c and l are the contact area and the length of the conductive fibers, respectively. The total measured resistance, R_T between the voltage probes is as follows:

$$R_T = R_v^{fiber} + R_c + R_v^{matrix} \quad (8)$$

Since conductivity of fibers is very high, R_v^{fiber} is negligible. By choosing a matrix that is small in dimension in the plane perpendicular to the fiber and choosing a matrix that is not too high in volume resistivity, R_v^{matrix} is negligible, so that equation (8) becomes

$$R_T = R_c \quad (9)$$

The contact resistivity of conductive fiber/cement composite was measured during curing process for 3 days. While the tensile load was applied continuously, the contact resistance and mechanical properties of the electro-pullout specimen was monitored simultaneously

2. 2. 4. AE Measurement: AE signals were detected using a miniature sensor (Resonance type, Physical Acoustics Co.) during electro-micromechanical pullout testing, and measured using a WD sensor (Broad Band type, PAC) for tensile/compressive tests. The sensor output was amplified by 40 dB at preamplifier, and the threshold level was set as 30-35 dB. The signal was fed into AE processing unit (MISTRAS 2001 system) and then AE parameters were analyzed (Figure 1). Typical AE parameters such as hit rate, peak amplitude and event energy were investigated in terms of testing time and distribution analysis. In order to obtain frequency characteristics, AE waveform was analyzed by in built program for fast *Fourier* transform (FFT).

3. RESULTS AND DISCUSSION

3. 1. Results of Electro-Pullout Test and AE: In Table 1, Electrical and the contact resistivity of carbon fiber composites were larger than those of steel fiber cases due to higher resistivity of carbon fiber. Comparing to the untreated for both steel and carbon fiber composites, the electrical and the contact resistivity of the treated case increased because Zr coupling agent acts as the insulator. The contact resistivity was the highest in the hand-sanded case. It might be due to micro-void that could act electrical insulator based on the insufficient wetting between fiber and cement.

Table 1 Resistivity properties of steel and carbon fiber/cement composite at the initial stage.

Fiber	Surface Condition	Electrical Resistance (Ω)	Electrical Resistivity (Ω·cm) × 10^{-4}	Contact Resistance (Ω)	Contact Resistivity ($\Omega \cdot cm^2$)
Steel	Untreated	0.57 (0.07)*	1.09 (0.14)	670.4 (19.4)	76.2 (2.2)
	Hand-sanded[1)]	0.59 (0.10)	1.10 (0.19)	1127.7 (53.7)	128.2 (6.1)
	Zr-Treated[2)]	0.62 (0.05)	1.16 (0.10)	740.4 (41.2)	84.2 (4.8)
Carbon	Untreated	1.57×10^3 (120)	12.5 (1.0)	650.1×10^3 (75.7×10^3)	12.9×10^6 (1.51×10^6)
	Zr-Treated	1.64×10^3 (224)	12.9 (1.8)	658.2×10^3 (89.2×10^3)	13.1×10^6 (1.77×10^6)

* Parenthesis is standard deviation.
* Electrical resistance of steel and carbon fibers was measured at gauge length in 32mm.
* Contact resistance of steel and carbon fiber/cement composites was at gauge length in 10 mm.
1) Hand-sanded with sand paper of #400
2) Treated by 7 wt% Zr-containing coupling agent ethanol solution

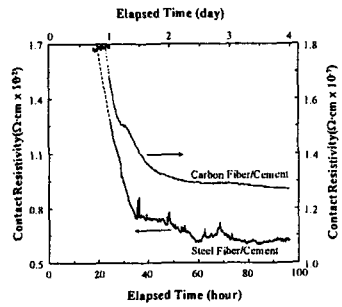

Fig. 2 Contact resistivity of steel and carbon fiber during curing process

Table 2 IFSS and the maximum load of steel and carbon fiber composites using electro-pullout test.

Fiber	Surface Condition	Diameter (μm)	Maximum Load (K_{gf})	IFSS[1)] (MPa)
Steel	Untreated	280	9.2 (0.3)*	10.3 (0.3)
	Hand-sanded	272	14.1 (0.6)	15.7 (0.7)
	Zr-treated	279	11.3 (0.4)	12.5(0.5)
Carbon	Untreated	18	0.051 (0.004)	4.43 (0.1)
	Zr-treated	18	0.047 (0.005)	4.12 (0.1)

* Parenthesis is standard deviation.
1) IFSS was calculated using equation (2).
2) Cannot measured

Figure 2 showed the contact resistivity with the elapsed time in the untreated steel and carbon fiber/cement composite during curing process. In both cases, the contact resistivity decreased abruptly at the initial stage, and then showed the level-off at the final stage. Solid line is the measured data, whereas dot line is the expecting data. In Table 2, IFSS of the hand-sanded steel fiber specimen is higher than both the untreated and Zr-treated cases, whereas that of the untreated specimen is the lowest. It might be considered that the effect of mechanical interlocking is larger than that of chemical functional group. IFSS of the untreated carbon fiber

composite is similar to that of Zr-treated case. Comparing to the steal fiber composites, the maximum stress is significantly lower due to the insufficient wetting at the interface between fiber and cement.

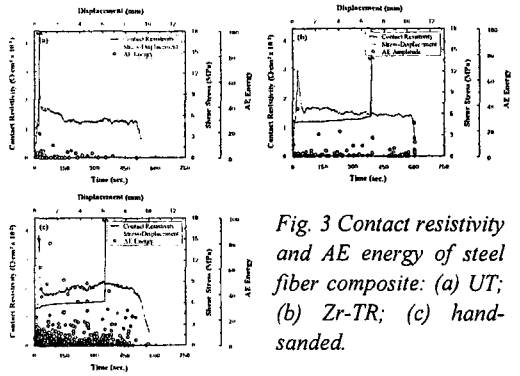

Fig. 3 Contact resistivity and AE energy of steel fiber composite: (a) UT; (b) Zr-TR; (c) hand-sanded.

Figure 3 showed the contact resistivity, AE energy, shear stress of steel fiber/cement composite depending on the surface treatment using electro-pullout test and AE. The contact resistivity of the untreated steel fiber composite increased suddenly at the initial stage, whereas those of Zr-treated and hand-sanded fiber cases increase at the latter stage. Although the fiber pulling-out occurred in Zr-treated and hand-sanded composites, the contact resistivity did not increase to the infinity. This could be considered that the interface was kept on contacting electrically, or showing the maintenance of partial electrical contact until further strain level. The number of AE signals of the hand-sanded steel fiber composite is much more than that of the untreated and Zr-treated cases. The maximum shear stress of the hand-sanded is larger than that of the untreated and Zr-treated case due to the mechanical interlocking.

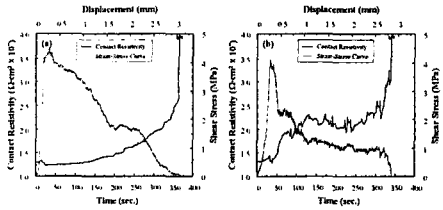

Fig. 4 Contact resistivity of (a) UT and (b) Zr-TR carbon fiber composite.

Figure 4 showed the contact reisistivity of the untreated and Zr-treated carbon fiber composites with testing time. In both carbon fiber composites, the contact resistivity increased slightly before the beginning to be pulled-out. This trend might be due to fiber dimensional change. At the next stage, the contact resistivity increased steadily in the untreated composite, whereas that increased stepwise in the Zr-treated composite. This might be because of the different interaction between fiber and cement due to surface treatment. Finally, the contact resistivity of carbon fiber composite increased to the infinity at the complete pullout state.

3. 2. Outcomes of DMC by Tensile/Compressive Tests: In Figure 5, AE event number of microfailure exhibited a relatively well-separated group in no-fiber and glass fiber composites using tensile and compressive tests. The event number of high amplitude in glass fiber composite was observed much more than that in no-fiber composite.

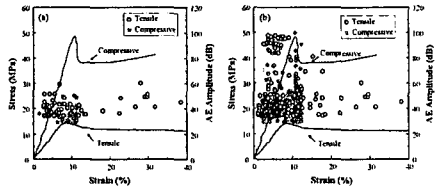

Fig. 5 AE amplitude and S-S curve of (a) no-fiber and (b) glass fiber composites.

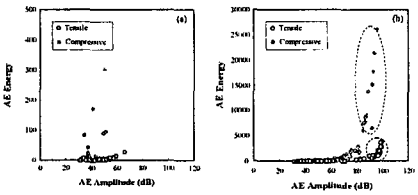

Fig. 6 AE amplitude versus AE energy curve of (a) no-fiber and (b) glass fiber composites.

In Figure 6(b), many AE signals due to breaking of glass fiber were observed in the region of high amplitude-energy comparing to no-fiber specimen (Figure 6(b)). In both no-fiber and glass fiber composites, AE energy under compressive loading was higher than that under tensile loading. It might be considered that the broken cement matrix was seems to behave continuous phase although many matrix crack occurred under compressive loading, so that the external stress could act on the fractured cement due to the increasing packing density. Under tensile loading, however, fracture energy might be expected to decrease with the increasing matrix crack, and then AE energy could decrease gradually.

Table 3 IFSS and brittle matrix crack spacing of glass fiber DMC using tensile fragmentation test.

Type	σ_{mu} (MPa)	Crack Spacing (μm)	IFSS[1)] (MPa)
Glass Fiber Composite	3.0	467	15.2
No-Fiber Composite	-[2)]	913	-

1) IFSS was calculated using equation (3)
2) Cannot measured

In Table 3, IFSS and brittle cement crack spacing of glass fiber reinforced composite are 15.2 MPa and 467 μm, respectively. Since IFSS does not exist in the no-

fiber composite, crack spacing of glass fiber composite is larger than that of no-fiber composite. It is due to the absence of fiber capable to endure the stress transferring.

In Figure 7(a) and (b), the vertical cracks were observed in glass fiber composite under tension, whereas diagonal cracks were observed in no-fiber composite. In Figure 7(c), buckling-shaped fractures were observed at the critical point on the stress concentration, and small-cracks was observed under the compressive testing.

Fig. 7 Photographs of cement composites: (a) glass fiber and (b) no-fiber (tensile); (c) glass fiber (compressive)

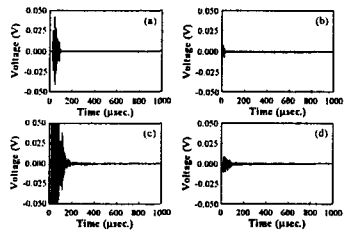

Fig. 8 AE waveforms of (a) the first pullout and (b) frictional (UT); (c) the first pullout and (d) frictional (hand-sanded).

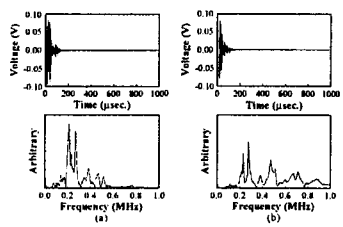

Fig. 9 AE waveforms and FFT of glass fiber composite under (a) tensile and (b) compressive test.

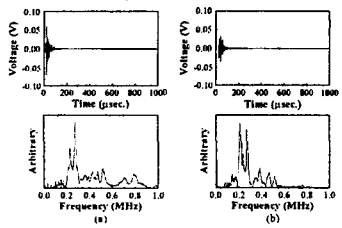

Fig. 10 AE waveforms and FFT of no-fiber composite by (a) tensile and (b) compressive test.

3. 3. AE Waveforms and Their FFT Analysis: AE waveform of the first pulled-out signal is larger than that of frictional signal in Figure 8. This might be due to the difference in microfailure mechanism depending on the interfacial adhesion. AE waveforms of the pulled-out and frictional signals in the hand-sanded case are larger than those in the untreated case. This trend might be considered that the interfacial failure was retarded due to the mechanical interlocking in the microspecimen having the higher IFSS. In Figure 9, characteristic peak coming from fiber breakage appeared mainly at near 0.2-0.3 MHz under tensile test. In compressive test, although characteristic peaks were similar to the tensile test, peak intensity increases in the region of above 0.6 MHz. AE voltage of glass fiber composite under tensile load is relatively larger than that under compressive load. Many peaks exhibited at the range of below 0.6 MHz under compressive test, whereas the peaks showed at the nearly all range under tensile test (Figure 10).

4. CONCLUSIONS

During curing process, the contact resitivity of micro-composites decreased abruptly at the initial stage and then showed the steady state. Comparing to the untreated steel fiber composite, the contact resistivity of Zr-treated and hand-sanded fiber composites increased to the infinity at the latter stage. The number of AE signals of hand-sanded steel fiber composite was much more than that of the other cases, due to the improved IFSS. Many signals in high amplitude in glass fiber composite were observed compared to the no-fiber composite. Vertical and diagonal cracks exhibited in glass fiber and no-fiber composite under tensile load, whereas buckling-shaped failure was also observed in glass fiber composite under compressive load. AE waveforms of the pulled-out and frictional signals in the hand-sanded case are larger than those in the untreated case. Electro-micromechanical test and AE can be a useful method to evaluate nondestructively microfailure mechanisms of various conductive fibers/brittle cement matrix composites.

ACKNOWLEDGEMENT: This study was supported financially by Korea Research Institute of Standards and Science (KRISS).

REFERENCES

(1) T. Okabe, N. Takeda, J. Komotori, M. Shimizu, and W. A. Curtin, *Acta Mater.*,vol. 47, 1999, pp. 4299-4309.
(2) W. A. Curtin, *J. Am. Ceram. Soc.*, vol. 74, 1991, pp. 2837-2845.
(3) S. I. Lee, J. M. Park, D. W. Shin, and D. J. Yoon, *Polymer Compos.*, vol. 20, 1999, pp. 19-28.
(4) C. Ageorges, K. Friedrich, T. Schuller, and B. Lauke, *Composite Part A*, vol. 30, 1999, pp. 1423-1434.
(5) X. Fu, D. D. L. Chung, *Compos. Interfaces*, vol. 4, 1998, pp. 197-211.
(6) J. M. Park, W. G. Shin, and D. J. Yoon, *Compos. Sci. & Technol.*, vol. 59, 1999, pp. 355-370.